Human Mesenchymal Stem Cell Delivery System Modulates Ischemic Cardiac Remodeling With an Increase of Coronary Artery Blood Flow

Young Sook Lee[1], Wan Seok Joo[2], Hyun Soo Kim[2] and Sung Wan Kim[1,3]

[1]Center for Controlled Chemical Delivery (CCCD), Department of Pharmaceutics and Pharmaceutical Chemistry, University of Utah, Salt Lake City, Utah, USA; [2]Pharmicell Co., Ltd., Sungnam, Republic of Korea; [3]Department of Bioengineering, Hanyang University, Seoul, Republic of Korea

Ways for extending the longevity of stem cells are imperative to attain diverse expected therapeutic effects. Here, we constructed a three-dimentional (3D) scaffold system for human mesenchymal stem cell (hMSC) delivery. Intramyocardial injections of porous $PEI_{1.8k}$ blended with poly(lactic-co-glycolic acid) (PLGA) ($PLGA/PEI_{1.8k}$) (PPP) microparticles by physical electrostatic conjugation and structural entrapment of hMSCs demonstrated enhanced functional and geometric improvements on post-infarct cardiac remodeling in rats. In the hMSC-loaded PPP delivery, increases of coronary artery blood flow rate and *in vivo* engraftment rate as well as time-dependent functional, geometric, and pathologic findings reversing post-infarct cardiac remodeling account for improved left ventricular (LV) systolic function up to the level of sham thoracotomy group. This study expands our understanding by proving that increase of coronary artery blood flow augmented functional recovery of hMSC-loaded PPP delivery system after myocardial infarction (MI).

Received 2 June 2015; accepted 10 January 2016; advance online publication 1 March 2016. doi:10.1038/mt.2016.22

INTRODUCTION

With huge burden of the direct medical cost, myocardial infarction (MI) caused by coronary artery disease (CAD) is the leading cause of morbidity and mortality worldwide.[1–7] Over the past five decades, reperfusion of the occluded infarct-related artery by early percutaneous coronary intervention (PCI) has been the standard treatment modality for minimizing infarct size and maintaining ventricular performance.[8] However, the process of restoring blood flow to the ischemic myocardium, termed myocardial reperfusion injury, can paradoxically even increase infarct size and partially explain the most common postinfarct morbidity, heart failure, and mortality.[2,9] As a result of these converging influences, we are at a crucial juncture where novel cardioprotective and reparative strategies for reversing cellular and molecular mechanisms responsible for postinfarct cardiac remodeling are solely needed.[10–14]

Mesenchymal stem cells (MSCs) have the multipotent potential mediated via combined paracrine, endocrine, and homing actions, including amelioration of inflammatory manifestation, modulation of immune response, mitogenics, antiapoptotic and anti-inflammatory effects, and stimulation of vasculogenesis and angiogenesis.[15–18] Diverse potent organ-protective effects of human MSCs render it one of the most likely candidates for the elusive physiological shield against disease, trauma, and aging. However, accompanied with lengthy *ex vivo* processing for 3–4 weeks, the low rate of engraftment and homing after human MSC (hMSC) transplantation is a major drawback to accomplish higher *in vivo* therapeutic efficiency.

A temporary anchoring with 3D structures is often investigated to support the proliferation and differentiation of cells by providing both appropriate physical and chemical environments.[19] Especially, a 3D porous scaffold for providing a large surface area and mass transports of nutrients and oxygen for cell attachment and proliferation imparts numerous advantages. Preliminary work suggested that hMSC-loaded porous microparticles can preserve greatly enhanced *in vivo* engraftment rate of hMSCs in infarcted myocardium over a 2-week period after intramyocardial injections than hMSC-alone group,[20] but its efficacy at modulating ischemic cardiac cascade had not been tested. To date, little is known about how biodegradable 3D hMSC delivery system, compared with hMSC-alone, distinctly alters cardiac remodeling in the rat MI model. Here, we report the sustained and augmented efficacy of hMSC delivered by biodegradable porous microparticles on functional, hemodynamic, and pathologic levels of cardiac ischemic cascade for reversing adverse cardiac remodeling after MI. We demonstrate the feasibility of our delivery system acting as a cell depot at the extracellular cardiac matrix potentially applicable to basic and translational studies.

RESULTS

hMSC delivery system improves LV systolic function and preserves cardiac geometry

To examine the hypothesis that delivery of hMSC-loaded PPP microparticles affects time-dependent functional and geometric ischemic cascades in heart, we first performed transthoracic echocardiography 1 and 4 weeks after MI. On postinfarct week 1, the administration of both hMSC-alone and hMSC-loaded PPP microparticles showed an improved left ventricular ejection fraction (LVEF) and the LV diameter during the systolic and diastolic phase comparable to the sham thoracotomy group (**Figure 1a,b**).

Correspondence: Sung Wan Kim, Center for Controlled Chemical Delivery (CCCD), Department of Pharmaceutics and Pharmaceutical Chemistry, University of Utah, Salt Lake City, Utah, USA. E-mail: (sw.kim@pharm.utah.edu)

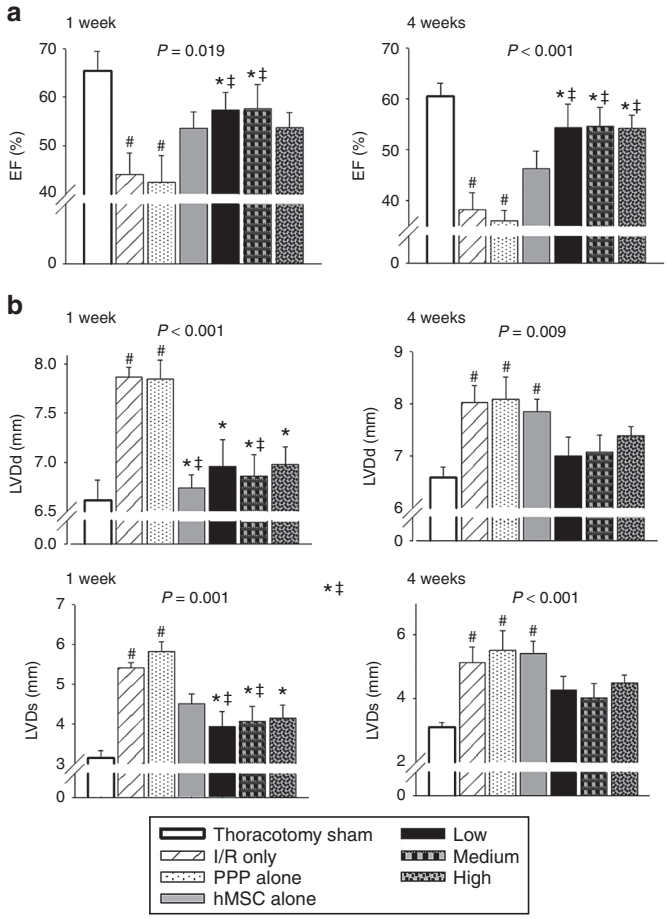

Figure 1 Time-dependent functional and geometric effects on postinfarct cardiac remodeling 1 week and 4 weeks after myocardial infarction. Male Sprague–Dawley (SD) rats received intramyocardial injections with a total volume of 200 µl right after I/R in left anterior descending coronary artery; sham thoracotomy, I/R only, PPP particle-alone, human mesenchymal stem cell (hMSC)-alone (2×10^6 hMSCs), PPP particles loaded with three different amounts of hMSC. The hMSC-loaded PPP particle groups were administered with three different hMSC amounts at 1 mg of PPP particle: 20×10^5 (high group), 10×10^5 (medium group), and 5×10^5 (low group). Data represent means ± SEM with n = 7–9 per group. (**a**) Systolic function evaluated by ejection fraction (%) of LV. (**b**) LV dimension during diastole (LVDd) and systole (LVDs). #P < 0.05 versus sham thoracotomy, *P < 0.05 versus I/R, ‡P < 0.05 versus PPP particle-alone, §P < 0.05 versus hMSC-alone.

However, this reserved functional and geometric improvements were remarkable sustained only in the hMSC-loaded PPP group up to the level of the thoracotomy group on postinfarct week 4 (**Figure 1a**,**b**). The post wall thickness, interventricular septum thickness, and LV mass during the systolic and diastolic phase did not reveal any differences between the groups on both 1 and 4 weeks (data not shown). All of the echocardiographic parameters of the PPP-alone injection group were comparable to the I/R-only group, excluding the impact of the PPP microparticle itself.

hMSC delivery system augments blood flow of coronary artery

The evaluation of coronary microvascular function by transthoracic Doppler echocardiography is addressed as a seminal therapeutic target.[21–24] The blood flow of the proximal left anterior descending (LAD) coronary artery showed a characteristic biphasic blood flow pattern with a larger diastolic component and a small systolic one in spectral Doppler echocargiography (**Supplementary Figure S1**). hMSC-loaded PPP delivery system demonstrated increased diameter, total blood volume (measured by velocity time integral (VTI)), output, and stroke volume of coronary artery on postinfarct week 4 (**Figure 2a**,**b**). These findings suggest an improvement on total blood volume, output, and stroke volume of coronary artery by hMSC-loaded PPP microparticle system that might be a potential mechanism to reversing postinfarct cardiac remodeling. This may elucidate in part, the beneficial effect of hMSC-loaded PPP delivery system on improving coronary microvascular dysfunction during postinfarct cardiac remodeling over time.

hMSC delivery system decreases cardiomyocyte loss and apoptotic activity

Next, we performed Immunohistochemical (IHC) staining of cardiomyocyte-specific cardiac troponin T (cTnT) of the rat heart myocardium 4 weeks after MI. The cardiomyocyte is the major cardiac cell involved in the cardiac remodeling process. The loss of cardiomyocytes after MI is the early distinctive pathologic finding. Compared with the I/R, and PPP particles-alone group, the hMSC-alone group and hMSC-loaded PPP groups showed significantly decreased cardiomyocytes loss (**Figure 3a**,**b**). Also, postinfarct cardiac remodeling contains diverse cellular changes, including apoptosis. Thus, we evaluated the effect against apoptotic activity in the border zone of LV infarct between groups. The apoptotic activity measured by TUNEL staining revealed lower apoptosis in the hMSC-loaded PPP group than that of the other groups (**Figure 3c**).

hMSC delivery system enhances angiogenesis and ameliorates cardiac fibrosis with a reduced infarct size

To recover cardiac function after MI, angiogenesis establishes the blood supply to the infarcted myocardium during the healing phase of postinfarct cardiac remodeling. IHC staining for α-SMA demonstrated more abundant arterioles in the hMSC-loaded PPP particles injection group than in the other treatment groups (**Figure 4a**,**b**), suggesting higher upregulation of angiogenic activity in the border zone of the infarct and potential enhanced oxygen supply to the infarcted myocardium. Especially, high amount of hMSC-loaded PPP group showed the most prominent upregulation of angiogenesis in the border zone of the infarct. Next, fibrosis is a common final pathological finding, resulted from diseases of heart as well as many organs. The loss of myocardial muscle mass caused by fibrotic scar formation is related to heart failure, the most common postinfarct morbidity. We evaluated whether the intramyocardial injections of hMSC-loaded PPP particles had an effect in the suppression of cardiac fibrosis on post-infarct cardiac remodeling. In Masson's trichrome staining of collagen, the postinfarct fibrotic scar areas in the mid-LV of the hMSC-loaded PPP particles groups were comparable to the sham thoracotomy group (**Figure 4c**,**d**). Compared with the I/R and PPP particles-alone group, the hMSC-alone group and hMSC-loaded PPP

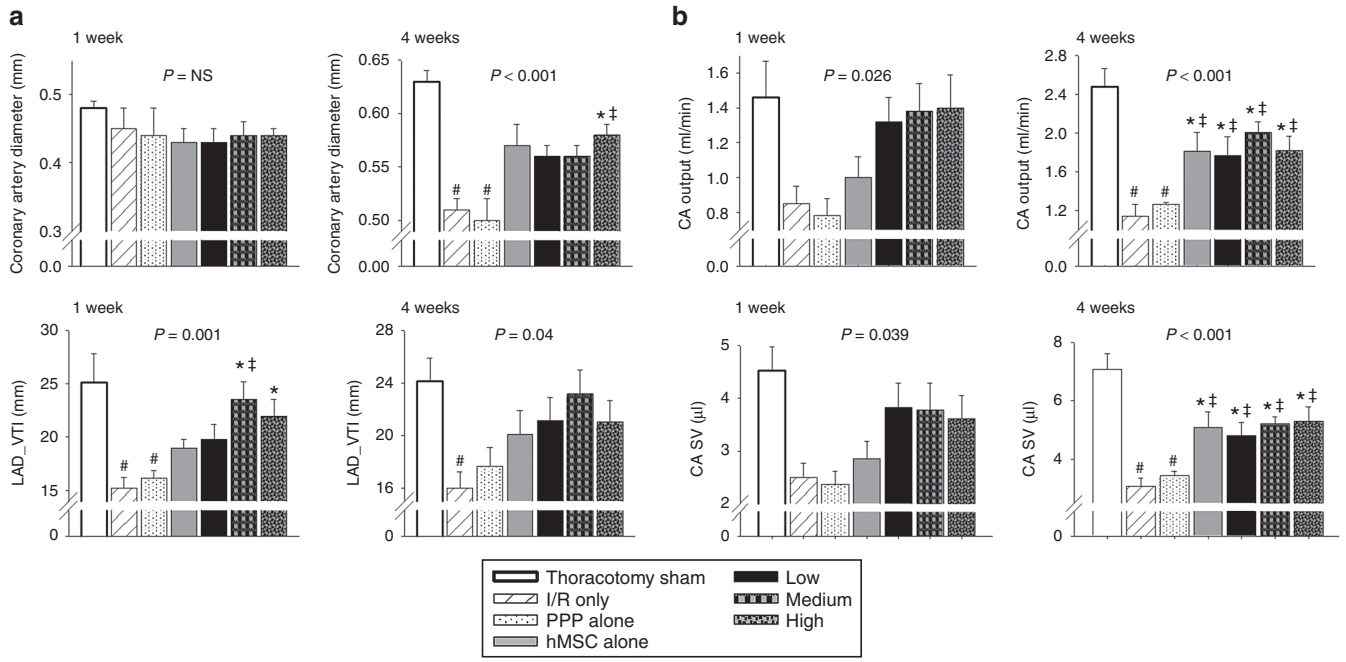

Figure 2 Hemodynamic improvements of coronary artery blood flow on postinfarct cardiac remodeling 1 week and 4 weeks after myocardial infarction. (**a**) Diameter of coronary artery and total blood volume measured by velocity time integral of left anterior descending (LAD) coronary artery (LAD_VTI). (**b**) Coronary artery (CA) output (ml/min) and CA stroke volume (SV) (µl) measured at the proximal LAD. Data represent means ± SEM with $n = 7–9$ per group. #$P < 0.05$ versus sham thoracotomy, *$P < 0.05$ versus I/R, ‡$P < 0.05$ versus PPP particle-alone, §$P < 0.05$ versus hMSC-alone. LAD, left anterior descending.

groups showed significantly decreased fibrotic area in the mid-LV (**Figure 4c,d**). Together with our study, we assume that the extended stability of hMSC loaded on PPP microparticles in the ischemic cardiac tissue exerts prolonged paracrine effects, enough to reverse the functional, geometric, hemodynamic, and pathologic remodeling process after MI.

DISCUSSION

hMSC delivered by biodegradable porous microparticles demonstrated prolonged and enhanced cardioprotective effects on reversing adverse postinfarct cardiac remodeling in functional, geometric, pathologic, and hemodynamic levels, especially by exerting an increase of coronary artery blood flow. Several deliberations for more potent and sustained functional improvement by hMSC-loaded PPP delivery system are possible. First, the proximal compartment of the coronary arterial system has a capacitance function and little resistance to coronary blood flow.[21] We observed increased diameter and total blood volume (VTI) of proximal LAD coronary artery on postinfarct week 4, possibly inducing an enhanced capacitance function of coronary blood flow and improved oxygen supply to ischemic myocardium.

Second, MI is caused by obstructive atherosclerosis of the epicardial coronary arteries.[21] However, the association between the severity and extent of coronary artery disease and clinical manifestations has often demonstrated no direct correlation.[25] Here, coronary microvascular dysfunction, defined as abnormalities in the function and structure of the coronary microcirculation can be epiphenomena in some clinical conditions.[21] Whereas, in others, coronary microvascular dysfunction may provide a pivotal clue predicting clinical outcome of coronary artery disease and cardiomyopathy, contribute to the pathogenesis of cardiac ischemic remodeling, and evaluate the effects of adjunct therapies.[21] The function of coronary microvasculature is evaluated by the indirect quantification of blood flow through the coronary circulation and expressed in milliliters per minute.[21] In clinic, coronary microvascular dysfunction is assessed by transthoracic Doppler echocardiography, intracoronary measurement, myocardial position-emission tomography imaging, or cardiovascular magnetic resonance (CMR).[21–24] In addition, the coronary flow velocity reserve (CFVR) was defined as the ratio of hyperemic to basal peak or mean diastolic coronary flow velocity.[26] The CFVR in the infarct-related artery after MI is regarded as the most valuable prognostic parameter, priming for early occurrence of heart failure and recovery of LV function.[22] And the CFVR in the remote reference coronary artery is related to the long-term outcome, independent of LV function.[22] This hMSC-loaded PPP delivery system augmented output and stroke volume of proximal LAD coronary artery on postinfarct week 4. Our results suggest that the hMSC-loaded PPP delivery system as well as hMSC-alone therapy potentiate to recover coronary microvascular dysfunction followed by MI on postinfarct week 4.

Third, LVEF is a representative functional parameter and powerful prognostic predictor after MI.[27,28] Furthermore, the combination of lower LVEF and severe stenosis of coronary artery exhibited higher risk of mortality.[29] So far, the functional and prognostic significances of coronary microvascular dysfunction need to be more investigated, especially correlated with LVEF. In our study, the combined consideration of LV and coronary artery function may provide better understanding for the promising effects of the hMSC-loaded PPP delivery system.

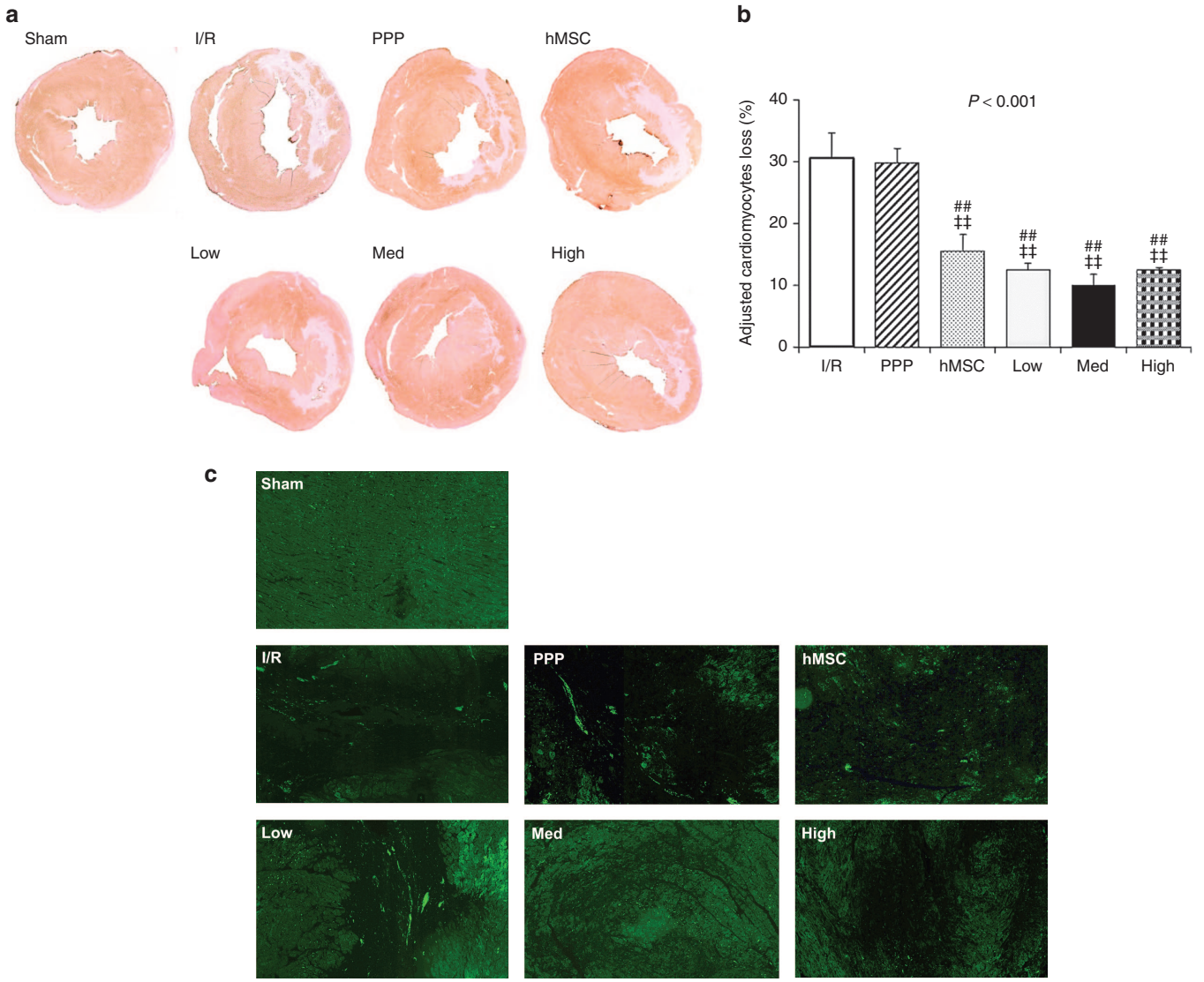

Figure 3 hMSC-loaded PPP delivery system alleviates cardiomyocytes loss and apoptotic activity 4 weeks after myocardial infarction. (**a**) Representative IHC staining images of cardiomyocyte-specific cardiac troponin T (cTnT) in the mid-LV of hearts from each group. (**b**) Quantification of percent cardiomyocytes loss in the LV adjusted by the level of thoracotomy group (mean ± SEM, $n = 7–9$ per group). $^{**}P < 0.01$ versus I/R, $^{*}P < 0.05$ versus I/R, $^{\ddagger\ddagger}P < 0.01$ versus PPP particle-alone, $^{\ddagger}P < 0.05$ versus PPP particle-alone. (**c**) Representative TUNEL-staining images in the border zone of LV infarct from each group (5× magnification, $n = 7–9$ per group).

Fourth, hMSC exerts the multipotent therapeutic effects via combined paracrine, endocrine, and homing actions.[15–17] Nowdays, many studies give bigger weigh to paracrine effects of hMSCs than homing action itself. In our result, the intramyocardial injection of hMSC-alone did not reach any significant histopathologic effects. The placement of hMSC-alone may not guarantee that hMSCs induce the therapeutic paracrine effects as well as sustain the engraftment efficiency. In our previous study, hMSC-loaded porous microparticles demonstrated the increased *in vivo* engraftment rate of hMSCs and the conserved stemness characteristics of hMSCs in the infarcted myocardium 2 weeks after intramyocardial injections than hMSC-alone group.[20] We speculated that the hMSC-loaded porous microparticles may provide the enhanced improvements on postinfarct cardiac remodeling due to the higher engraftment efficiency and derived prolonged paracrine action.

The biodegradable and bioabsorbable PLGA microspheres are able to degrade up to several months in aqueous environments like living tissues.[30,31] Infarcted myocardium has acidic tissue environment. The degradation of PLGA may alter the local microenvironment and influence structure and function in tissues.[31–33] Also, direct injections of same amount of DNA into heart showed 10–100 times higher expression of gene than into skeletal muscle, with a more limited distribution of gene expression.[28,34,35] Therefore, intramyocardial administration of hMSC-loaded PPP microsphere system may amplify and extend the therapeutic response at the local site with lowering systemic adverse side effects.[36] In the results, we can exclude the effect of PPP microparticle itself on postinfarct cardiac remodeling.

Sixth, hMSC-loaded PPP microsphere system revealed favorable pathologic cardiac remodeling after MI, including lower cardiomyocyte loss and apoptotic activity, higher angiogenic activity,

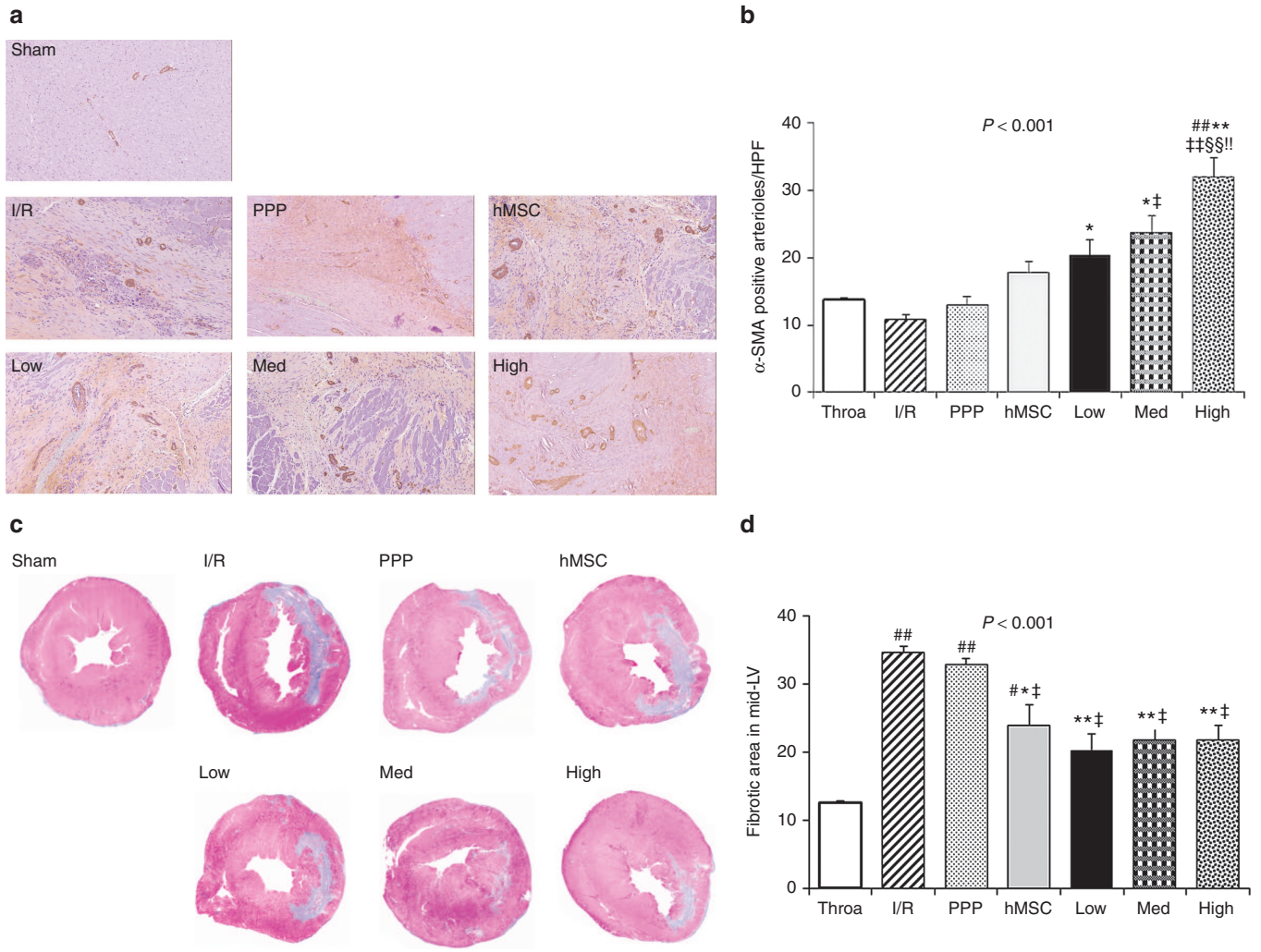

Figure 4 The prolonged engraftment of hMSC-loaded PPP delivery system induces angiogenesis and suppresses postinfarct fibrosis 4 weeks after myocardial infarction. (**a**) Representative IHC-staining images of the α-SMA-postive arterioles (10× magnification). (**b**) Quantification of proangiogenic activity by the α-SMA-positive arterioles (mean ± SEM, $n = 7–9$ per group, three to five images per heart). $^{\#\#}P < 0.01$ versus sham thoracotomy, $^{**}P < 0.01$ versus I/R, $^{*}P < 0.05$ versus I/R, $^{\ddagger\ddagger}P < 0.01$ versus PPP particle-alone, $^{\ddagger}P < 0.05$ versus PPP particle-alone, $^{\S\S}P < 0.01$ versus hMSC-alone, $^{!!}P < 0.01$ versus low amount of hMSC-loaded PPP. (**c**) Representative Masson's trichrome staining images in the mid-LV of hearts from each group. (**d**) Quantification of percent fibrosis area in LV (mean ± SEM, $n = 7–9$ per group). $^{\#\#}P < 0.01$ versus sham thoracotomy, $^{\#}P < 0.05$ versus sham thoracotomy, $^{**}P < 0.01$ versus I/R, $^{*}P < 0.05$ versus I/R, $^{\ddagger}P < 0.05$ versus PPP particle-alone. hMSC, human mesenchymal stem cell.

and smaller cardiac fibrosis and infarct size. This favorable pathologic recovery in hMSC-loaded PPP microsphere system may allow the delivered hMSCs to sustain in more intact cardiac extracellular matrix, resulting in stronger and prolonged cardioprotective effects after MI.

This study had some limitations. In spite of a vigorous research on hMSC, we still do not know the complete therapeutic mechanisms of hMSC in many diseases. In this study, we tried to expand the understanding of therapeutic effects of hMSC-loaded PPP delivery system on postinfarct cardiac remodeling, especially in the view of coronary microvascular hemodynamics. However, this study did not provide diverse molecular mechanisms of hMSC-loaded PPP delivery system to explain the enhanced therapeutic effects after MI in rats. The fundamental and extensive studies of hMSCs in the molecular and cellular levels are requisite to advance the diverse clinical application. Generally, Followed the stunning and hibernating of myocardium in first week after MI, the myocardium was remodeled in days to months. The long-term evaluation of functional and histopathologic measurements can provide powerful supports of this hMSC-loaded PPP delivery system on post-MI remodeling. However, the technical hurdle of our setting in echocardiography was hard to evaluate the several months follow-up. The transthoracic echocardiography is a standard diagnostic tool in the clinics to get many information by experts. However, compared with the cardiac magnetic resonance imaging (MRI), the transthoracic echocardiography is affected by the subjective skill of examiner as well as hemodynamic parameters under the anesthesia.

Overall, our study demonstrates that this biodegradable 3D scaffold can enhance and amplify the therapeutic efficacy of delivered hMSCs, attaining improved therapeutic goal during postinfarct cardiac remodeling. This biodegradable 3D microsphere-based hMSC delivery system promises a convenient and effective vehicle for the treatment of diverse debilitating and incurable diseases.

MATERIALS AND METHODS

Human MSC (hMSC). Human MSC transferred from the Pharmicell (Sungnam, South Korea) was used in this study as previously described.[20] The hMSC was characterized by flow cytometry (BD Biosciences), using specific positive surface markers CD105, CD73 and while being negative for hematopoietic markers such as CD34, CD45, and CD14. After thawing, hMSCs were cultured in low-glucose Dulbecco's modified Eagle's medium containing 10% fetal bovine serum, 20 μg/ml gentamicin in a humidified incubator at 37 °C under 5% CO_2.

Preparation of porous microparticles. The porous polyethylenimine (Mw 1,800, $PEI_{1.8k}$) blended with poly($_{D,L}$-lactic-co-glycolic acid) (PLGA) microparticles (PPP particles) were synthesized by a modified water/oil/water ($W_1/O/W_2$) double emulsion solvent evaporation method as previously described with an average particle size of 290 μm and an average pore size of 14.3 μm. The hMSCs and PPP particles were incubated for 24 hours using continuous agitation at 37 °C under 5% CO_2 to attach the cells. The next day, three different amounts of hMSC-loaded PPP particles were administered in rats.

Rat model of myocardial infarction and hMSC transplantation. MI was induced in male Sprague–Dawley (SD) rats (7–8 weeks old with a body weight of 220–250 g) by 30-minute surgical occlusion of the LAD coronary artery as previously described.[20,28] The animals were assigned to one of seven groups (each $n = 9$): (i) sham thoracotomy, (ii) I/R only, (iii) injection of PPP particle-alone, (iv) injection of hMSC-alone (2×10^6 hMSCs), (v–vii) injection of PPP particles loaded with three different amounts of hMSC. The hMSC-loaded PPP particle groups were administered with three different hMSC amounts at 1 mg of PPP particle: 20×10^5 (high group), 10×10^5 (medium group), and 5×10^5 (low group). Right after successful ischemia–reperfusion (I/R), the rats received a total injection volume of 200 μl delivered to four separate intramyocardial sites with three injections to the ischemic border zone of the infarct in LV (LVb) and one injection to the fibrotic central zone of the infarct in LV (LVc) with 23 1/4 gauze needle. Animals were followed for 4 weeks after intramyocardial transplantation.

Echocardiography. To assess LV remodeling and function in rats, transthoracic echocardiography was performed on weeks 1 and 4 after the intramyocardial administration in rats lightly anesthetized with isoflurane at 1–2 l/minute and spontaneous respiration. Echocardiograms were performed with a special small animal echocardiography system (Vevo2100 High-Resolution Imaging System, VisualSonics) equipped with a 13- to 24-MHz linear-array transducer (MS250, MS400 MicroScan Transducer, VisualSonics). Transthoracic coronary blood flow velocity in the proximal LAD coronary artery, infarct-related coronary artery was measured during diastole and systole 1 and 4 weeks after postinfarct intramyocardial injections (**Supplementary Figure S1a**,**b**). All measurements were averaged for three consecutive cardiac cycles.

Pathological analysis. Serial 4-μm-thick sections of rat myocardium were fixed, embedded, and stained with H&E stain. Fibrosis, determined by collagen contents was evaluated by Masson's trichrome stain. IHC staining was performed on the 4-μm-thick sections of formalin-fixed, paraffin-embedded rat hearts tissue. Sections were air-dried at room temperature and then placed in a 60 °C oven for 30 minutes to melt the paraffin. All of the staining steps were performed at 37 °C using an automated immunostainer (BenchMark XT, Ventana Medical Systems). To evaluate the loss of cardiomyocytes and angiogenesis, determined by the arteriolar density after MI, heart sections were IHC stained using α-smooth muscle actin (αSMA) and cardiomyocyte-specific troponin T (cTnT). The sections were detected using the ULTRAView DAB detection kit (Ventana Medical Systems). The sections were counterstained with hematoxylin for 8 minutes. Also, apoptosis by TUNEL positivity in the infarct border zones was evaluated as the number of terminal deoxynucleotidyltransferase (TdT)-labeled nuclei per a unit area. Analysis of all images was randomly chosen within the infarct border zone of LV and carried out in five random high-power fields per section using ImageScope (Aperio Technologies, Vista, CA).

Statistical analysis. All data were expressed as mean ± SEM. Comparisons between multiple groups were performed by analysis of variance followed by Tukey *post-hoc* testing. A P value < 0.05 was considered statistically significant.

SUPPLEMENTARY MATERIAL

Figure S1. Representative spectral Doppler images of proximal LAD coronary artery in transthoracic echocardiography.

ACKNOWLEDGMENTS

The authors thank Pharmicell Co., Ltd., for providing hMSC. The authors also thank Sheryl R. Tripp and Blake K. Anderson (ARUP Institute for Clinical & Experimental Pathology, Salt Lake City, UT) for the histological and IHC staining. This work was supported by the University of Utah Small Animal Ultrasound Core Facility in addition to the NIH National Center for Research through Award Number 1S10RR027506-01A01.

REFERENCES

1. Lloyd-Jones, D, Adams, RJ, Brown, TM, Carnethon, M, Dai, S, De Simone, G *et al.* (2010). Heart disease and stroke statistics--2010 update: a report from the American Heart Association. *Circulation* **121**: e46–e215.
2. Yellon, DM and Hausenloy, DJ (2007). Myocardial reperfusion injury. *N Engl J Med* **357**: 1121–1135.
3. Deb, S, Wijeysundera, HC, Ko, DT, Tsubota, H, Hill, S and Fremes, SE (2013). Coronary artery bypass graft surgery vs percutaneous interventions in coronary revascularization: a systematic review. *JAMA* **310**: 2086–2095.
4. Gaziano, TA, Bitton, A, Anand, S, Abrahams-Gessel, S and Murphy, A (2010). Growing epidemic of coronary heart disease in low- and middle-income countries. *Curr Probl Cardiol* **35**: 72–115.
5. Mathers, CD and Loncar, D (2006). Projections of global mortality and burden of disease from 2002 to 2030. *PLoS Med* **3**: e442.
6. Murray, CJ and Lopez, AD (1997). Alternative projections of mortality and disability by cause 1990-2020: Global Burden of Disease Study. *Lancet* **349**: 1498–1504.
7. Heidenreich, PA, Trogdon, JG, Khavjou, OA, Butler, J, Dracup, K, Ezekowitz, MD *et al.*; American Heart Association Advocacy Coordinating Committee; Stroke Council; Council on Cardiovascular Radiology and Intervention; Council on Clinical Cardiology; Council on Epidemiology and Prevention; Council on Arteriosclerosis; Thrombosis and Vascular Biology; Council on Cardiopulmonary; Critical Care; Perioperative and Resuscitation; Council on Cardiovascular Nursing; Council on the Kidney in Cardiovascular Disease; Council on Cardiovascular Surgery and Anesthesia, and Interdisciplinary Council on Quality of Care and Outcomes Research. (2011). Forecasting the future of cardiovascular disease in the United States: a policy statement from the American Heart Association. *Circulation* **123**: 933–944.
8. Opie, LH, Commerford, PJ, Gersh, BJ and Pfeffer, MA (2006). Controversies in ventricular remodelling. *Lancet* **367**: 356–367.
9. Windecker, S, Bax, JJ, Myat, A, Stone, GW and Marber, MS (2013). Future treatment strategies in ST-segment elevation myocardial infarction. *Lancet* **382**: 644–657.
10. Spinale, FG and Zile, MR (2013). Integrating the myocardial matrix into heart failure recognition and management. *Circ Res* **113**: 725–738.
11. Sanganalmath, SK and Bolli, R (2013). Cell therapy for heart failure: a comprehensive overview of experimental and clinical studies, current challenges, and future directions. *Circ Res* **113**: 810–834.
12. Shah, AM and Mann, DL (2011). In search of new therapeutic targets and strategies for heart failure: recent advances in basic science. *Lancet* **378**: 704–712.
13. Du, XJ, Bathgate, RA, Samuel, CS, Dart, AM and Summers, RJ (2010). Cardiovascular effects of relaxin: from basic science to clinical therapy. *Nat Rev Cardiol* **7**: 48–58.
14. González, A, Ravassa, S, Beaumont, J, López, B and Díez, J (2011). New targets to treat the structural remodeling of the myocardium. *J Am Coll Cardiol* **58**: 1833–1843.
15. Pittenger, MF, Mackay, AM, Beck, SC, Jaiswal, RK, Douglas, R, Mosca, JD *et al.* (1999). Multilineage potential of adult human mesenchymal stem cells. *Science* **284**: 143–147.
16. Giordano, A, Galderisi, U and Marino, IR (2007). From the laboratory bench to the patient's bedside: an update on clinical trials with mesenchymal stem cells. *J Cell Physiol* **211**: 27–35.
17. Parekkadan, B and Milwid, JM (2010). Mesenchymal stem cells as therapeutics. *Annu Rev Biomed Eng* **12**: 87–117.
18. Bagul, A, Frost, JH and Drage, M (2013). Stem cells and their role in renal ischaemia reperfusion injury. *Am J Nephrol* **37**: 16–29.
19. Choi, S-W, Zhang, Y, Yeh, Y-C, Wooten, AL and Xia, Y (2012). Biodegradable porous beads and their potential applications in regenerative medicine. *J Mater Chem* **22**: 11442–11451.
20. Lee, YS, Lim, KS, Oh, JE, Yoon, AR, Joo, WS, Kim, HS *et al.* (2015). Development of porous PLGA/PEI1.8k biodegradable microspheres for the delivery of mesenchymal stem cells (MSCs). *J Control Release* **205**: 128–133.

21. Camici, PG and Crea, F (2007). Coronary microvascular dysfunction. *N Engl J Med* **356**: 830–840.
22. van de Hoef, TP, Bax, M, Meuwissen, M, Damman, P, Delewi, R, de Winter, RJ, *et al.* (2013). Impact of coronary microvascular function on long-term cardiac mortality in patients with acute ST-segment-elevation myocardial infarction. *Circ Cardiovasc Interv* **6**: 207–215.
23. Fang, F, Jin, ZN, Li, HY, Zhang, WJ, Li, ZA, Yang, Y *et al.* (2014). Left anterior descending coronary artery flow impaired by right ventricular apical pacing: the role of systolic dyssynchrony. *Int J Cardiol* **176**: 80–85.
24. Cortigiani, L, Rigo, F, Gherardi, S, Galderisi, M, Bovenzi, F and Sicari, R (2014). Prognostic meaning of coronary microvascular disease in type 2 diabetes mellitus: a transthoracic Doppler echocardiographic study. *J Am Soc Echocardiogr* **27**: 742–748.
25. de Silva, R and Camici, PG (1994). Role of positron emission tomography in the investigation of human coronary circulatory function. *Cardiovasc Res* **28**: 1595–1612.
26. Hozumi, T, Yoshida, K, Ogata, Y, Akasaka, T, Asami, Y, Takagi, T *et al.* (1998). Noninvasive assessment of significant left anterior descending coronary artery stenosis by coronary flow velocity reserve with transthoracic color Doppler echocardiography. *Circulation* **97**: 1557–1562.
27. Traverse, JH, Henry, TD and Moye', LA (2011). Is the measurement of left ventricular ejection fraction the proper end point for cell therapy trials? An analysis of the effect of bone marrow mononuclear stem cell administration on left ventricular ejection fraction after ST-segment elevation myocardial infarction when evaluated by cardiac magnetic resonance imaging. *Am Heart J* **162**: 671–677.
28. Lee, Y, McGinn, AN, Olsen, CD, Nam, K, Lee, M, Shin, SK *et al.* (2013). Human erythropoietin gene delivery for cardiac remodeling of myocardial infarction in rats. *J Control Release* **171**: 24–32.
29. Min, JK, Lin, FY, Dunning, AM, Delago, A, Egan, J, Shaw, LJ *et al.* (2010). Incremental prognostic significance of left ventricular dysfunction to coronary artery disease detection by 64-detector row coronary computed tomographic angiography for the prediction of all-cause mortality: results from a two-centre study of 5330 patients. *Eur Heart J* **31**: 1212–1219.
30. Ford Versypt, AN, Pack, DW and Braatz, RD (2013). Mathematical modeling of drug delivery from autocatalytically degradable PLGA microspheres–a review. *J Control Release* **165**: 29–37.
31. van Apeldoorn, AA, van Manen, HJ, Bezemer, JM, de Bruijn, JD, van Blitterswijk, CA and Otto, C (2004). Raman imaging of PLGA microsphere degradation inside macrophages. *J Am Chem Soc* **126**: 13226–13227.
32. Nickerson, MM, Song, J, Shuptrine, CW, Wieghaus, KA, Botchwey, EA and Price, RJ (2009). Influence of poly(D,L-lactic-co-glycolic acid) microsphere degradation on arteriolar remodeling in the mouse dorsal skinfold window chamber. *J Biomed Mater Res A* **91**: 317–323.
33. Sung, HJ, Meredith, C, Johnson, C and Galis, ZS (2004). The effect of scaffold degradation rate on three-dimensional cell growth and angiogenesis. *Biomaterials* **25**: 5735–5742.
34. Dean, DA (2005). Nonviral gene transfer to skeletal, smooth, and cardiac muscle in living animals. *Am J Physiol Cell Physiol* **289**: C233–C245.
35. Kitsis, RN, Buttrick, PM, McNally, EM, Kaplan, ML and Leinwand, LA (1991). Hormonal modulation of a gene injected into rat heart in vivo. *Proc Natl Acad Sci USA* **88**: 4138–4142.
36. Zolnik, BS and Burgess, DJ (2008). Evaluation of in vivo-in vitro release of dexamethasone from PLGA microspheres. *J Control Release* **127**: 137–145.